Progress In Electromagnetics Research, PIER 102, 65–80, 2010

PARAMETERIZATION OF THE TILTED GAUSSIAN BEAM WAVEOBJECTS

Y. Hadad and T. Melamed

Department of Electrical and Computer Engineering
Ben-Gurion University of the Negev
Beer Sheva 84105, Israel

Abstract—Novel time-harmonic beam fields have been recently obtained by utilizing a non-orthogonal coordinate system which is *a priori* matched to the field's planar linearly-phased Gaussian aperture distribution. These waveobjects were termed tilted Gaussian beams. The present investigation is concerned with parameterization of these time-harmonic tilted Gaussian beams and of the wave phenomena associated with them. Specific types of tilted Gaussian beams that are characterized by their aperture complex curvature matrices, are parameterized in term of beam-widths, waist-locations, collimation-lengths, radii of curvature, and other features. Emphasis is placed on the difference in the parameterization between the conventional (orthogonal coordinates) beams and the tilted ones.

1. INTRODUCTION

Beam-type expansion of scalar or electromagnetic fields has gain much attention in the past several years owing to their mutual spectral and spatial localization which result in local interactions between the beam fields and the propagating/scattering medium. This feature is significantly advantageous for propagation and scattering and results in simplified analytic expressions for the beam fields. Locality considerations have been utilized for solving beam-type waveobjects propagation in generic media profiles such as inhomogeneous [1–3], anisotropic [4–11], and for time-dependent pulsed beams, in dispersive media [12–16].

The need for beam solutions arises from beam-type (phase-space) expansions such as Gabor-based expansions [17, 18] or the frame-based field expansion [19, 20]. The latter utilizes the overcompleteness

Corresponding author: T. Melamed (timormel@ee.bgu.ac.il).

nature of the beam's continuous spectrum [18, 21, 22], and discretizes the spectral representation with no loss of essential data for reconstruction. A theoretical overview of frame-based representation of scalar time-harmonic fields is presented in [19], with an extension to electromagnetic fields in [23], and for time-dependent scalar fields in [20].

Exact beam-type expansions require beam solutions that match localized aperture planar distributions. In these solutions the boundary plane over which the aperture field distribution is given is generally *not perpendicular* to the beam direction of propagation (the beam-axis). Therefore, in order to use conventional (orthogonal coordinates) Gaussian beams, apart from asymptotic approximations an additional approximation is carried out to project the aperture field complex curvature matrix on a plane *normal* to the beam-axis direction. This additional approximation reduces the accuracy of the resulting beam solutions especially for large angle departures and, moreover, it becomes *inconsistent with respect to asymptotic orders*. The need for the additional approximation can be avoided by using the recently introduced tilted GBs which are localized beam-type solutions to the Helmholtz equation [24]. These waveobjects are matched to linearly-phased Gaussian aperture field distributions over a plane which is tilted with respect to the corresponding beam-axes.

The present paper deals with the properties and parameterization of tilted Gaussian beams (GBs) and the additional wave phenomena associated with applying a non-orthogonal coordinate system. These waveobjects are parameterized in terms of spatial widths, wave-front radii of curvature, collimation lengths, and other features. Since such waveobjects serve as the basic building blocks for different beam-type expansions, it is an important task to parameterize them in order to utilize these expansion schemes in different scattering scenarios [25–34].

2. TILTED GAUSSIAN BEAMS

A discrete exact expansion scheme which synthesizes the EM field propagating in $z \geq 0$ due to sources in $z < 0$ was presented in [23, 24]. The electric field expansion is described by a superposition of EM beam propagators which emanate from a set of discrete points over the $z = 0$ aperture plane in a discrete set of directions. This set of directions is determined by introducing a linear phase term $\exp[-jk(\bar{\xi}_1 x_1 + \bar{\xi}_2 x_2)]$ in which $\bar{\boldsymbol{\xi}} = (\bar{\xi}_1, \bar{\xi}_2)$ are the expansion (directional) spectral variables. The EM vectorial beam propagators are obtained directly from the *scalar tilted GBs* subject to a transverse shift over the aperture to the spectral expansion lattice.

The tilted GBs are identified by aperture planar distributions over the $z = 0$ plane of the form

$$B_0(\mathbf{x}) = \exp\left[-jk\left(\bar{\boldsymbol{\xi}}^T\mathbf{x} + \frac{1}{2}\mathbf{x}^T\boldsymbol{\Gamma}_0\,\mathbf{x}\right)\right], \tag{1}$$

where $k = \omega/v_0$ is the homogeneous medium wavenumber with v_0 being the medium wave speed. Here and henceforth, all fields carry a suppressed time-dependence of $\exp(j\omega t)$, all vectors are column vectors, superscript T is used to denote matrix or vector transpose, bold minuscule letters are used to denote column vectors and bold capital letters are used to denote matrices. The aperture complex curvature matrix, $\boldsymbol{\Gamma}_0$, is a 2×2 complex symmetrical matrix with a negative definite imaginary part. Note that Eq. (1) is comprised of a Gaussian distribution with a linear phase-term which causes the beam to tilt with respect to the $z = 0$ plane.

The tilted GBs in [24] were obtained by introducing a novel *non-orthogonal* coordinate system which is *a priori* matched to distribution (1). In this system $\mathbf{r}_b = (x_{b_1}, x_{b_2}, z_b)$ where the z_b-axis is in the beam-axis propagation direction and the transverse coordinates, x_{b_1} and x_{b_2}, lie on a plane parallel to the (x_1, x_2) plane and are centered at its intersection with the z_b-axis (see Fig. 1). The transformation

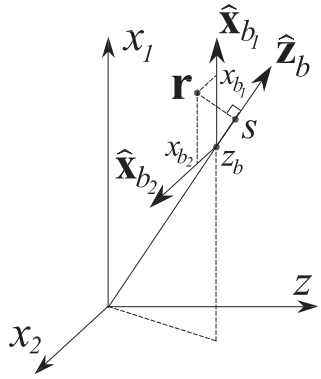

Figure 1. Non-orthogonal local beam coordinate system. Observation point $\mathbf{r} = (x_{b_1}, x_{b_2}, z_b)$ where z_b is the origin location along the paraxial propagation direction, $\hat{\mathbf{z}}_b$, and the transverse coordinates, x_{b_1} and x_{b_2}, lie on a plane parallel to the (x_1, x_2) plane. Thus, the transverse coordinates are tilted with respect to the propagation direction $\hat{\mathbf{z}}_b$.

from $\mathbf{r} = (x_1, x_2, z)$ to $\mathbf{r}_b = (x_{b_1}, x_{b_2}, z_b)$ is given by

$$\mathbf{r}_b = \begin{bmatrix} 1 & 0 & -\bar{\xi}_1/\bar{\zeta} \\ 0 & 1 & -\bar{\xi}_2/\bar{\zeta} \\ 0 & 0 & \bar{\zeta}^{-1} \end{bmatrix} \mathbf{r}, \quad \mathbf{r} = \begin{bmatrix} 1 & 0 & \bar{\xi}_1 \\ 0 & 1 & \bar{\xi}_2 \\ 0 & 0 & \bar{\zeta} \end{bmatrix} \mathbf{r}_b, \tag{2}$$

where the longitudinal (normalized) spectral wavenumber $\bar{\zeta} = \sqrt{1 - \bar{\xi}_1^2 - \bar{\xi}_2^2}$, and the observation vector is given by

$$\mathbf{r}_b = x_{b_1}\hat{\mathbf{x}}_{b_1} + x_{b_2}\hat{\mathbf{x}}_{b_2} + z_b\hat{\mathbf{z}}_b, \tag{3}$$

with $\hat{\mathbf{x}}_{b_1}, \hat{\mathbf{x}}_{b_2}$ and $\hat{\mathbf{z}}_b$ denoting the unit-vectors in the direction of the x_{b_1}, x_{b_2} and z_b axes, respectively. Note that $\hat{\mathbf{x}}_{b_1} = \hat{\mathbf{x}}_1$, $\hat{\mathbf{x}}_{b_2} = \hat{\mathbf{x}}_2$, whereas $\hat{\mathbf{z}}_b = (\bar{\boldsymbol{\xi}}, \bar{\zeta})$. Here and henceforth, a hat over a vector denotes a unit-vector.

The asymptotically-exact tilted GB solutions are given by

$$B(\mathbf{r}_b) = \sqrt{\frac{\det \boldsymbol{\Gamma}(z_b)}{\det \boldsymbol{\Gamma}_0}} \exp[-jk\Psi(\mathbf{r}_b)], \;\; \Psi(\mathbf{r}_b) = s(\mathbf{r}_b) + \frac{1}{2}\mathbf{x}_b^T \boldsymbol{\Gamma}(z_b)\, \mathbf{x}_b, \tag{4}$$

where $\mathbf{x}_b = (x_{b_1}, x_{b_2})$, the Eikonal (see Fig. 1)

$$s(\mathbf{r}_b) = z_b + \bar{\xi}_1 x_{b_1} + \bar{\xi}_2 x_{b_2}, \tag{5}$$

and $\boldsymbol{\Gamma}(z_b)$ is given by

$$\boldsymbol{\Gamma}(z_b) = \left[\boldsymbol{\Gamma}_0^{-1} + \bar{\zeta}^{-2}\boldsymbol{\Psi} z_b\right]^{-1}. \tag{6}$$

$\boldsymbol{\Gamma}_0$ is the aperture complex curvature matrix of the field distribution in (1) and

$$\boldsymbol{\Psi} = \begin{bmatrix} \left(1 - \bar{\xi}_2^2\right) & \bar{\xi}_1\bar{\xi}_2 \\ \bar{\xi}_1\bar{\xi}_2 & \left(1 - \bar{\xi}_1^2\right) \end{bmatrix}. \tag{7}$$

The waveobjects in (4) exhibit a Gaussian decay away from the beam-axes over which $\mathbf{x}_b = 0$. Their properties are determined by the complex curvature matrices $\boldsymbol{\Gamma}(z_b)$, which are obtained from the aperture complex curvature matrices $\boldsymbol{\Gamma}_0$ in (1) via (6). The characteristics of these waveobjects vary with the aperture distribution features according to the main categories in the following section.

3. PROPERTIES OF TILTED GBS

3.1. Conventional (Orthogonal System) GB

The special case of a normally propagating GB is obtained by setting $\bar{\boldsymbol{\xi}} = 0$ in (2) and (7). Consequently, no linear phase is included in the aperture field distribution in (1) so that the resulting beam-axis

coincides with the z-axis. The paraxial beam coordinate system in (2) is orthogonal (i.e., $(x_{b_1}, x_{b_2}, z_b) = (x_1, x_2, z)$) and the beam field in (4) transforms into the well-known conventional beam solution [2, 35]

$$B(\mathbf{r}) = \sqrt{\frac{\det \mathbf{\Gamma}(z)}{\det \mathbf{\Gamma}_0}} \exp\left\{-jk\left[z + \frac{1}{2}\mathbf{x}^T \mathbf{\Gamma}(z)\mathbf{x}\right]\right\}, \tag{8}$$

where

$$\mathbf{\Gamma}(z_b) = \left[\mathbf{\Gamma}_0^{-1} + z_b \mathbf{I}\right]^{-1}. \tag{9}$$

with $\mathbf{I}$ denoting the 2×2 unity matrix.

In order to clarify the characteristics of the GB in (8), we rotate the transverse coordinates $\mathbf{x}$ in order to diagonalize $\mathbf{\Gamma}(z)$. Any *real* 2×2 symmetric matrix, $\mathbf{\Gamma} = \{\Gamma_{i,j}\}$, can be diagonalized by a rotation matrix of the form

$$\mathbf{x}_c = \mathbf{T}_c \mathbf{x}, \quad \mathbf{T}_c = \begin{bmatrix} \cos\Phi_c & \sin\Phi_c \\ -\sin\Phi_c & \cos\Phi_c \end{bmatrix}, \tag{10}$$

where

$$\tan(2\Phi_c) = 2\Gamma_{1,2}/(\Gamma_{1,1} - \Gamma_{2,2}), \tag{11}$$

so that the quadratic phase in (8) is given by

$$\mathbf{x}^T \mathbf{\Gamma} \mathbf{x} = \mathbf{x}_c^T \mathbf{\Gamma}_c \, \mathbf{x}_c, \quad \mathbf{\Gamma}_c = \mathbf{T}_c \mathbf{\Gamma} \mathbf{T}_c^{-1}, \tag{12}$$

with $\mathbf{\Gamma}_c$ being a *diagonal* matrix. However, in the general case in which $\mathbf{\Gamma}$ is complex, the two real symmetric matrices, Re$\mathbf{\Gamma}$ and Im$\mathbf{\Gamma}$, cannot be diagonalized *simultaneously*. Therefore, we define two rotation angles, Φ_r and Φ_j, that yield two principal axes, $\mathbf{x}_r = \mathbf{T}_r \mathbf{x}$ and $\mathbf{x}_j = \mathbf{T}_j \mathbf{x}$, in which Re$\mathbf{\Gamma}$ and Im$\mathbf{\Gamma}$ are diagonalized, respectively. Note that the rotation angles, Φ_r and Φ_j, are in general z-dependent. Nevertheless, in the special case in which the principal axes, $\mathbf{x}_r$ and $\mathbf{x}_j$ coincide at the beam origin $z = 0$, it follows that the axes coincide for all z values and the rotation angle becomes independent of z. The GB waveobject in this particular case was previously termed *iso-axial* [2]. The conventional (orthogonal system) GB and its time-dependent counterpart, the pulsed beam, have been well studied in [2, 22] and [36]. Here we present the results concerning the *iso-axial* GB, but a more general case can be easily parameterized in a similar manner. While investigating the properties of the iso-axial GB, it is sufficient to consider the case of a diagonal aperture matrix $\mathbf{\Gamma}_0$, since any other (iso-axial) aperture matrix can be rotated and diagonalized in the $z = 0$ plane following the procedure in (10)–(12). Denoting

$$\mathbf{\Gamma}_0 = \mathrm{diag}\left\{(-Z_1 + jF_1)^{-1}, (-Z_2 + jF_2)^{-1}\right\}, \quad F_{1,2} > 0, \tag{13}$$

the complex curvature matrix in (9) is given by

$$\mathbf{\Gamma}(z) = \begin{bmatrix} (z - Z_1 + jF_1)^{-1} & 0 \\ 0 & (z - Z_2 + jF_2)^{-1} \end{bmatrix}. \tag{14}$$

By separating $\mathbf{\Gamma}(z)$ into its real and imaginary parts, we obtain

$$\mathrm{Re}\mathbf{\Gamma} = \mathrm{diag}\left\{R_1^{-1}(z), R_2^{-1}(z)\right\}, \ \mathrm{Im}\mathbf{\Gamma} = -\mathrm{diag}\left\{I_1^{-1}(z), I_2^{-1}(z)\right\}, \tag{15}$$

where

$$R_{1,2}(z) = (z - Z_{1,2}) + \frac{F_{1,2}^2}{(z - Z_{1,2})}, \ I_{1,2}(z) = F_{1,2}\left[1 + \frac{(z - Z_{1,2})^2}{F_{1,2}^2}\right]. \tag{16}$$

By inserting Eq. (16) with (14) into (8), $R_{1,2}(z)$ are identified as the *phase-front radii of curvature* on the principal axes. The e^{-1} *beam-widths* in $(x_{1,2}, z)$ principle planes are given by

$$W_{1,2}(z) = D_{1,2}\sqrt{1 + \frac{(z - Z_{1,2})^2}{F_{1,2}^2}}, \tag{17}$$

where $D_{1,2} = \sqrt{8F_{1,2}/k}$ is identified as the *principal beam waists* (see Fig. 2). We identify $F_{1,2}$ and $Z_{1,2}$ as the *beam collimation-lengths* and the *beam waist-locations* on the $(z, x_{c1,2})$ principal planes, respectively. Note that near the waist, $|z - Z_{1,2}| \ll F_{1,2}$, the GB remains collimated with approximately constant beam-widths $D_{1,2}$, whereas far from the waist, $|z - Z_{1,2}| \gg F_{1,2}$, the GB opens up along constant diffraction angles $\Theta_{1,2} = (kF_{1,2}/8)^{-1/2}$.

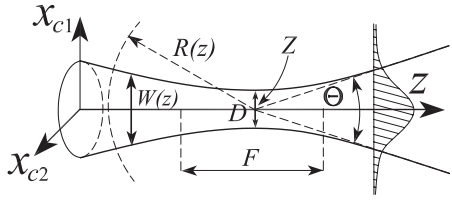

Figure 2. Parameterization of the conventional GB. The parameters are depicted over the (x_{c1}, z) plane. The tilted GB exhibits a Gaussian decay over constant z planes. $W(z)$ denotes the beam-widths, $R(z)$ the phase-front radius of curvature, D the width at the waist which are located in $z = Z$, F the collimation length and Θ denotes the far-field diffraction angle.

3.2. Iso-axial Tilted GB

Applying radially-symmetric Gaussian windows to an aperture field distribution results in a beam-type expansion scheme in which the propagating waveobjects are *iso-axial* tilted GBs. These GBs are characterized by a diagonal aperture complex curvature matrix of the form [19, 22, 23]

$$\mathbf{\Gamma}_0 = \mathbf{I}\Gamma_0, \quad \Gamma_0 = (-Z + jF)^{-1}, \quad F > 0. \tag{18}$$

The complex curvature matrix in this case is obtained by using (18) in (6), yielding

$$\mathbf{\Gamma}(z_b) = \begin{bmatrix} (1-\bar{\xi}_2^2)\bar{\zeta}^{-2}z_b - Z + jF & \bar{\xi}_1\bar{\xi}_2\bar{\zeta}^{-2}z_b \\ \bar{\xi}_1\bar{\xi}_2\bar{\zeta}^{-2}z_b & (1-\bar{\xi}_1^2)\bar{\zeta}^{-2}z_b - Z + jF \end{bmatrix}^{-1}. \tag{19}$$

Next we separate $\mathbf{\Gamma}(z_b)$ into its real and imaginary parts, i.e., $\mathbf{\Gamma} = \mathbf{\Gamma}_r + j\mathbf{\Gamma}_j$ with

$$\mathbf{\Gamma}_r = \begin{bmatrix} \Delta_r\left[\left(1-\bar{\xi}_1^2\right)\bar{\zeta}^{-2}z_b - Z\right] - \Delta_j F & -\Delta_r\bar{\xi}_1\bar{\xi}_2\bar{\zeta}^{-2}z_b \\ -\Delta_r\bar{\xi}_1\bar{\xi}_2\bar{\zeta}^{-2}z_b & \Delta_r\left[\left(1-\bar{\xi}_2^2\right)\bar{\zeta}^{-2}z_b - Z\right] - \Delta_j F \end{bmatrix}, \tag{20}$$

and

$$\mathbf{\Gamma}_j = \begin{bmatrix} \Delta_j\left[\left(1-\bar{\xi}_1^2\right)\bar{\zeta}^{-2}z_b - Z\right] + \Delta_r F & -\Delta_j\,\bar{\xi}_1\bar{\xi}_2\bar{\zeta}^{-2}z_b \\ -\Delta_j\bar{\xi}_1\bar{\xi}_2\bar{\zeta}^{-2}z_b & \Delta_j\left[\left(1-\bar{\xi}_2^2\right)\bar{\zeta}^{-2}z_b - Z\right] + \Delta_r F \end{bmatrix}, \tag{21}$$

where

$$\Delta_r = \frac{\delta_r}{\delta_r^2 + \delta_j^2}, \qquad \Delta_j = \frac{\delta_j}{\delta_r^2 + \delta_j^2}, \tag{22}$$

with

$$\begin{aligned} \delta_r &= Z^2 - F^2 - Z\left(1 + \bar{\zeta}^{-2}\right)z_b + \bar{\zeta}^{-2}z_b^2, \\ \delta_j &= -2ZF + F\left(1 + \bar{\zeta}^{-2}\right)z_b. \end{aligned} \tag{23}$$

Note that unlike in the conventional GB in Section 3.1, a diagonal aperture complex curvature matrix $\mathbf{\Gamma}_0$, results in a *non-diagonal* complex curvature matrix along z_b. The real and imaginary parts of the complex iso-axial curvature matrix can be diagonalized simultaneously by rotating the $\mathbf{x}_b$-axes over constant z_b-planes by a z_b-*independent* angle Φ_c, i.e., $\mathbf{x}_c = \mathbf{T}\mathbf{x}_b$. Then using (20) or (21) in (11), we obtain

$$\tan 2\Phi_c = 2\bar{\xi}_1\bar{\xi}_2 / \left(\bar{\xi}_1^2 - \bar{\xi}_2^2\right), \tag{24}$$

i.e., $\cos\Phi_c = \bar{\xi}_1/\bar{\xi}$ and $\sin\Phi_c = \bar{\xi}_2/\bar{\xi}$, where $\bar{\xi} = \sqrt{\bar{\xi}_1^2 + \bar{\xi}_2^2}$. Angle Φ_c is identified as the angle between the x_1-axis and the projection of

the z_b-axis on (x_1, x_2) plane. The resulting rotation transformation is given in (10). Finally, using (19) in (12), we obtain

$$\mathbf{\Gamma}_c(z_b) = \begin{bmatrix} \left(z_b\bar{\zeta}^{-2} - Z + jF\right)^{-1} & 0 \\ 0 & (z_b - Z + jF)^{-1} \end{bmatrix}, \tag{25}$$

for which Z and F are given in (18).

3.2.1. Beam-widths and Diffraction Angles

In order to parameterize the tilted iso-axial GB field, we separate the diagonalized complex curvature matrix $\mathbf{\Gamma}_c(z_b)$ into its real and imaginary parts by denoting

$$\mathrm{Re}\mathbf{\Gamma}_c = \mathbf{L}_c^{-1}(z_b), \qquad \mathrm{Im}\mathbf{\Gamma}_c = -\mathbf{I}_c^{-1}(z_b). \tag{26}$$

Then using (25), we obtain

$$\mathbf{L}_c(z_b) = \begin{bmatrix} \bar{\zeta}^{-2}\left[(z_b - Z_1) + \frac{F_1^2}{(z_b - Z_1)}\right] & 0 \\ 0 & \left[(z_b - Z_2) + \frac{F_2^2}{(z_b - Z_2)}\right] \end{bmatrix}, \tag{27}$$

and

$$\mathbf{I}_c(z_b) = \begin{bmatrix} F\left[1 + \frac{(z_b - Z_1)^2}{F_1^2}\right] & 0 \\ 0 & F\left[1 + \frac{(z_b - Z_2)^2}{F_2^2}\right] \end{bmatrix}, \tag{28}$$

with

$$Z_1 = Z\bar{\zeta}^2, \quad Z_2 = Z, \qquad F_1 = F\bar{\zeta}^2, \quad F_2 = F\,. \tag{29}$$

Using (26) with (28) in (4), we find that the iso-axial tilted GB exhibits (pure) quadratic decay in the (x_{c_1}, x_{c_2}) directions with corresponding

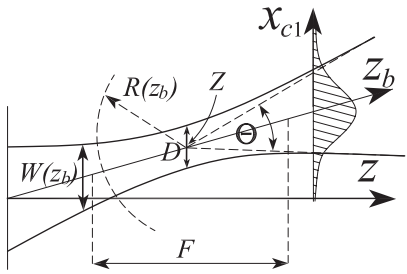

Figure 3. Parameterization of the iso-axial tilted GB. The field exhibits a Gaussian decay in the $\mathbf{x}_c$ coordinates. As in Fig. 2, the parameters are depicted over the $(x_{c1},\, z)$ plane.

e^{-1} beam-widths of

$$W_{1,2}(z_b) = D_{1,2}\sqrt{1 + \frac{(z_b - Z_{1,2})^2}{F_{1,2}^2}}, \tag{30}$$

where $D_{1,2} = \sqrt{8F_{1,2}/k}$ are the principal beam-widths at the waists. By using (30), we identify $F_{1,2}$ and $Z_{1,2}$ as the beam's *collimation-lengths* and the beam's *waist-locations* on the $(z_b, x_{c_{1,2}})$ principal planes, respectively. On the $(z_b, x_{c_{1,2}})$ planes, the beam field remains collimated near the waists where $|z_b - Z_{1,2}| \ll F_{1,2}$, whereas away from the waists, it opens up along constant diffraction angles of $\Theta_{1,2} = (kF_{1,2}/8)^{-1/2}$ in the $x_{c_{1,2}}$ axes (see Fig. 3). This type of Gaussian beam waveobjects exhibits frequency independent collimation (Rayleigh) lengths for which reason we previously termed it to be *iso-diffracting* [37]. This iso-diffracting feature makes such waveobjects highly suitable for UWB radiation representations [11, 13, 14, 38].

3.2.2. Phase-front Radii of Curvature

In order to parameterize the phase phenomenology as prescribed by the field quadratic phase-term $\exp[-jk\frac{1}{2}\mathbf{x}_b^T\mathbf{\Gamma}_r(z_b)\mathbf{x}_b]$ in *non-orthogonal* coordinates, we cast it in the *paraxial geometrical optics* ray-field

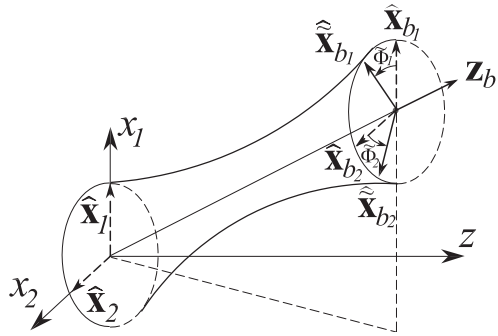

Figure 4. Rotated coordinates for phase-front radii of curvature evaluation. $\tilde{x}_{b_{1,2}}$ are rotated by angles $\tilde{\Phi}_{1,2}$ with respect to the beam transverse axes $x_{b_{1,2}}$. The rotation is carried out in the transverse coordinates plane (x_{b1}, x_{b2}) so that the projections of $\hat{\tilde{\mathbf{x}}}_{b_{1,2}}$ on the normal (to the beam-axis) plane (not shown in the figure) are orthogonal.

canonical form in *orthogonal* coordinates, namely [39]

$$B(\mathbf{r}) = \sqrt{\frac{R_1}{s+R_1}}\sqrt{\frac{R_2}{s+R_2}}\exp\left\{-jk\left[s+\frac{1}{2}\left(\frac{x_{n_1}^2}{s+R_1}+\frac{x_{n_2}^2}{s+R_2}\right)\right]\right\}. \quad (31)$$

Here, as in (5), s is the trajectory arclength, $R_{1,2}$ denotes the phase-front main radii of curvature at $s = 0$ and $\mathbf{x}_n = (x_{n_1}, x_{n_2})$ are orthogonal coordinates in the plane transverse to the ray direction $\hat{\mathbf{s}}$. The $\hat{\mathbf{z}}_b$-axis in waveobject in (4) is identified as the ray trajectory direction $\hat{\mathbf{s}}$. Next we relate the real part of the non-orthogonal complex curvature matrix to the ray central phase-front radii of curvatures $R_{1,2}(z_b)$. Note that the projections of $\mathbf{x}_n$ on the *tilted* aperture plane, (x_{b_1}, x_{b_2}), are *not orthogonal*. Therefore, we define new transverse coordinates in the direction of these projections, $\tilde{\mathbf{x}}_b = (\tilde{x}_{b_1}, \tilde{x}_{b_2})$, which are obtained from $\mathbf{x}_b$ by the on-plane transformation (see Fig. 4) as follows:

$$\tilde{\mathbf{x}}_b = \tilde{\mathbf{T}}\mathbf{x}_b, \quad \tilde{\mathbf{T}} = \begin{bmatrix} \cos\tilde{\Phi}_1 & \sin\tilde{\Phi}_1 \\ -\sin\tilde{\Phi}_2 & \cos\tilde{\Phi}_2 \end{bmatrix}. \quad (32)$$

Thus, $\tilde{x}_{b_{1,2}}$ are obtained by rotating the $x_{b_{1,2}}$ axes in the $\mathbf{x}_b$ plane by $\tilde{\Phi}_{1,2}$, respectively. Note that angles $\tilde{\Phi}_{1,2}$ are clockwise positive and that $|\tilde{\Phi}_{1,2}| < \pi/2$. By using (32) in (5) the tilted beam linear phase-term in the $\tilde{\mathbf{x}}_b$ system takes the form

$$s(\mathbf{r}_b) = z_b + \bar{\xi}_1 x_{b_1} + \bar{\xi}_2 x_{b_2} = z_b + \bar{\boldsymbol{\xi}}^T\tilde{\mathbf{T}}^{-1}\tilde{\mathbf{x}}_b, \quad (33)$$

whereas the paraxial term reads

$$\mathbf{x}_b^T\boldsymbol{\Gamma}_r\mathbf{x}_b = \tilde{\mathbf{x}}_b^T\tilde{\boldsymbol{\Gamma}}_r\tilde{\mathbf{x}}_b, \quad \tilde{\boldsymbol{\Gamma}}_r = \tilde{\mathbf{T}}^T\boldsymbol{\Gamma}_r\tilde{\mathbf{T}}, \quad (34)$$

where $\boldsymbol{\Gamma}_r(z_b)$ is given in (20). The rotation angles are chosen such that (a) the real part of the resulting rotated complex curvature matrix, $\tilde{\boldsymbol{\Gamma}}_r(z_b)$, is *diagonal* and (b) the projections of axes $\tilde{x}_{b_{1,2}}$ on the *normal plane* of constant s are *orthogonal* (as in (31)).

By setting the off-diagonal elements of $\tilde{\boldsymbol{\Gamma}}_r$ to zero, we obtain

$$\sin\tilde{\Phi}_1\cos\tilde{\Phi}_2\Gamma_{r_{11}} - \cos\tilde{\Phi}_1\sin\tilde{\Phi}_2\Gamma_{r_{22}} - \cos\left(\tilde{\Phi}_1+\tilde{\Phi}_2\right)\Gamma_{r_{12}} = 0, \quad (35)$$

for which the $\Gamma_{r_{mn}}$ elements of $\boldsymbol{\Gamma}_r$ are given in (20).

In order to meet condition (b), we project unit-vectors $\hat{\tilde{\mathbf{x}}}_{b_{1,2}}$ on the plane normal to $\hat{\mathbf{z}}_b$ and set the projections dot-product to zero. This procedure yields

$$\sin\left(\tilde{\Phi}_1 - \tilde{\Phi}_2\right) = \cos\tilde{\vartheta}_1\cos\tilde{\vartheta}_2, \quad (36)$$

where $\cos\tilde{\vartheta}_{1,2}$ are the angles between the z_b-axis and $\tilde{x}_{b_{1,2}}$ axes, respectively, i.e.,

$$\cos\tilde{\vartheta}_{1,2} = \hat{\mathbf{x}}_{b_{1,2}}\cdot\hat{\mathbf{z}}_b, \quad (37)$$

with unit-vectors

$$\begin{aligned}\hat{\tilde{\mathbf{x}}}_{b_1} &= \cos\tilde{\Phi}_1\hat{\mathbf{x}}_{b_1} + \sin\tilde{\Phi}_1\hat{\mathbf{x}}_{b_2},\\ \hat{\tilde{\mathbf{x}}}_{b_1} &= -\sin\tilde{\Phi}_2\hat{\mathbf{x}}_{b_1} + \cos\tilde{\Phi}_2\hat{\mathbf{x}}_{b_2}.\end{aligned} \tag{38}$$

Thus, the transverse rotation angles, $\tilde{\Phi}_{1,2}$, are obtained by solving (35) with (36). Then using angles $\tilde{\Phi}_{1,2}$ in (32) and applying (34), we obtain

$$\tilde{\mathbf{\Gamma}}_r(z_b) = \mathrm{diag}\{\lambda_1, \lambda_2\}, \tag{39}$$

with

$$\begin{aligned}\begin{bmatrix}\lambda_1\\ \lambda_2\end{bmatrix} &= \sec^2\left(\tilde{\Phi}_1 - \tilde{\Phi}_2\right)\\ &\times\left(\Gamma_{r_{11}}\begin{bmatrix}\cos^2\tilde{\Phi}_2\\ \sin^2\tilde{\Phi}_1\end{bmatrix} \pm\Gamma_{r_{12}}\begin{bmatrix}\sin 2\tilde{\Phi}_2\\ \sin 2\tilde{\Phi}_1\end{bmatrix} +\Gamma_{r_{22}}\begin{bmatrix}\sin^2\tilde{\Phi}_2\\ \cos^2\tilde{\Phi}_1\end{bmatrix}\right),\end{aligned} \tag{40}$$

and the quadratic phase in (34) taking the form

$$\frac{1}{2}\tilde{\mathbf{x}}_b^T\tilde{\mathbf{\Gamma}}_r\tilde{\mathbf{x}}_b = \frac{1}{2}\left(\lambda_1\tilde{x}_{b_1}^2 + \lambda_2\tilde{x}_{b_2}^2\right). \tag{41}$$

Finally, we sample the phase term in (41) and (33) on a plane *normal* to the ray trajectory (the beam-axis) which passes through z_b. Recalling that $x_{n_{1,2}}$ are the (orthogonal) coordinates in the direction of the projections of $\tilde{x}_{b_{1,2}}$, respectively (see (32)), it follows that for observation points over the normal plane $x_{n_{1,2}} = \tilde{x}_{b_{1,2}}\sin\tilde{\vartheta}_{1,2}$. By inserting the latter into (41) and (33), the (real) phase-term of the tilted GB field takes the paraxial GO canonical form

$$\Psi_r = s(z_b) + \frac{1}{2}\left[\frac{x_{n_1}^2}{R_1(z_b)} + \frac{x_{n_2}^2}{R_2(z_b)}\right], \tag{42}$$

where

$$R_{1,2}(z_b) = \frac{1-\cos^2\tilde{\vartheta}_{1,2}}{\lambda_{1,2}}. \tag{43}$$

In view of (31), $R_{1,2}(z_b)$ in (43) are identified as the iso-axial tilted GB principal *phase-front radii of curvature*.

3.3. Hetero-axial Tilted GB

We conclude our analysis of the tilted GB parametrization with the special-case of a generic *diagonal* aperture complex curvature matrix. This matrix is obtained by expanding an aperture field using a frame where different Gaussian windows are applied to each of the $x_{1,2}$-axes. The more general case of a symmetric aperture complex curvature

matrix has not been shown to reveal any additional physical insight and hence is not presented here. We assume a generic *diagonal* aperture distribution of the form

$$\mathbf{\Gamma}_0 = \mathrm{diag}\left[\left(-Z_1 + jF_1\right)^{-1}, \left(-Z_2 + jF_2\right)^{-1}\right], \quad F_{1,2} > 0. \tag{44}$$

By inserting (44) into (6), we obtain

$$\mathbf{\Gamma}(z_b) = \begin{bmatrix} \left(1-\bar{\xi}_2^2\right)\bar{\zeta}^{-2}z_b - Z_1 + jF_1 & \bar{\xi}_1\bar{\xi}_2\bar{\zeta}^{-2}z_b \\ \bar{\xi}_1\bar{\xi}_2\bar{\zeta}^{-2}z_b & \left(1-\bar{\xi}_1^2\right)\bar{\zeta}^{-2}z_b - Z_2 + jF_2 \end{bmatrix}^{-1}. \tag{45}$$

Similar to the analysis is Section 3.2, we separate $\mathbf{\Gamma}$ into its real and imaginary parts

$$\mathbf{\Gamma}_r = \begin{bmatrix} \Delta_r\left[(1-\bar{\xi}_1^2)\bar{\zeta}^{-2}z_b - Z_2\right] - \Delta_j F_2 & -\Delta_r\bar{\xi}_1\bar{\xi}_2\bar{\zeta}^{-2}z_b \\ -\Delta_r\bar{\xi}_1\bar{\xi}_2\bar{\zeta}^{-2}z_b & \Delta_r\left[(1-\bar{\xi}_2^2)\bar{\zeta}^{-2}z_b - Z_1\right] - \Delta_j F_1 \end{bmatrix}, \tag{46}$$

and

$$\mathbf{\Gamma}_j = \begin{bmatrix} \Delta_j\left[(1-\bar{\xi}_1^2)\bar{\zeta}^{-2}z_b - Z_2\right] + \Delta_r F_2 & -\Delta_j\bar{\xi}_1\bar{\xi}_2\bar{\zeta}^{-2}z_b \\ -\Delta_j\bar{\xi}_1\bar{\xi}_2\bar{\zeta}^{-2}z_b & \Delta_j\left[(1-\bar{\xi}_2^2)\bar{\zeta}^{-2}z_b - Z_1\right] + \Delta_r F_1 \end{bmatrix}, \tag{47}$$

where

$$\Delta_r = \frac{\delta_r}{\delta_r^2 + \delta_j^2}, \qquad \Delta_j = \frac{-\delta_j}{\delta_r^2 + \delta_j^2}, \tag{48}$$

with δ_r and δ_j being the real and imaginary parts of $1/\det\mathbf{\Gamma}$, respectively. By using (45), δ_{rj} can be expressed explicitly as

$$\delta_r = Z_1Z_2 - F_1F_2 - \left[Z_1(1-\bar{\xi}_1^2) + Z_2\left(1-\bar{\xi}_2^2\right)\right]\bar{\zeta}^{-2}z_b + \bar{\zeta}^{-2}z_b^2, \tag{49}$$

and

$$\delta_j = \left[F_1\left(1-\bar{\xi}_1^2\right) + F_2\left(1-\bar{\xi}_2^2\right)\right]\bar{\zeta}^{-2}z_b - F_1Z_2 - F_2Z_1. \tag{50}$$

Unlike the case of the iso-axial waveobject, parameterization of the hetero-axial tilted GB requires separate diagonalization of matrices $\mathbf{\Gamma}_r$ and $\mathbf{\Gamma}_j$. For that purpose, we define two transverse coordinate systems for either $\mathbf{\Gamma}_r$ or $\mathbf{\Gamma}_j$, which are obtained from $\mathbf{x}_b$ by applying rotation transformations of the form in (10) by angles Φ_r or Φ_j, respectively. In view of (46), (47) and (11), they are given by

$$\tan 2\Phi_r = \frac{2\Delta_r\bar{\xi}_1\bar{\xi}_2\bar{\zeta}^{-2}z_b}{\Delta_r\left[-Z_1 + Z_2 + (\bar{\xi}_1^2 - \bar{\xi}_2^2)\bar{\zeta}^{-2}z_b\right] + \Delta_j\left(F_2 - F_1\right)}, \tag{51}$$

and

$$\tan 2\Phi_j = \frac{2\Delta_j\bar{\xi}_1\bar{\xi}_2\bar{\zeta}^{-2}z_b}{\Delta_j\left[-Z_1 + Z_2 + (\bar{\xi}_1^2 - \bar{\xi}_2^2)\bar{\zeta}^{-2}z_b\right] + \Delta_r\left(F_1 - F_2\right)}. \tag{52}$$

Note that unlike the iso-axial GB, here the rotation transformations are z_b-*dependent* so that the beam principal axes rotate along the beam-axis. The resulting exact expressions for the diagonalized matrices can be obtained by applying rotation matrix (10) with rotation angles Φ_j or Φ_r in (51) or (52). However, the results are not presented as they do not add any additional insight. Nevertheless, for sufficiently large z_b values,

$$z_b \gg \max(Z_1 + F_1, Z_2 + F_2), \tag{53}$$

the rotation angle $\Phi_r \to \Phi_c$, where Φ_c is the z_b-independent iso-axial aperture distribution rotation angle in (24). Note that unlike Φ_r, away from the aperture plane, $\Phi_j \to \Phi_c$ of (24) only for $F_1 = F_2$. Angle Φ_j defines the new rotated transverse coordinates according to (10), in which the beam exhibits (pure) Gaussian decay. For z_b values which satisfy condition (53), diagonalization of $\mathbf{\Gamma}_j(z_b)$ yields,

$$\mathbf{\Gamma}_j(z_b) \cong -z_b^{-2}\mathrm{diag}(I_1^{-1}, I_2^{-1}), \tag{54}$$

where I_1^{-1} and I_2^{-1} are constant and equal to the eigenvalues of $-z_b^2\mathbf{\Gamma}_j$ in the limit (53). In view of the $O(z_b^{-2})$ dependence of $\mathbf{\Gamma}_j$, we can conclude that away from the waists, the beam opens up along a constant diffraction angles of $\Theta_{1,2} = (8I_{1,2}/k)^{1/2}$ on the principal planes $(x_{b_{1,2}}, z_b)$, respectively.

4. CONCLUDING REMARKS

Parametrization of tilted GBs in homogeneous media was carried out for several special cases of aperture field distributions. The waveobjects were parameterized in terms of waist-locations, beam-widths, collimation-lengths, and other wave features. The field principle radii of curvature were formulated to relate non-orthogonal beam components to conventional GO ray-fields in orthogonal coordinates. Understanding tilted GBs phenomena in term of the above parameters is significant for tuning up beam-type expansions for identifying and obtaining local interactions with scattering and complex media.

REFERENCES

1. Ĉerveny, V., M. M. Popov, and I. Pŝenĉik, "Computation of wave fields in inhomogeneous media — Gaussian beam approach," *Geophys. J. Roy. Asro. Soc.*, Vol. 70, 109–128, 1982.
2. Heyman, E., "Pulsed beam propagation in an inhomogeneous medium," *IEEE Trans. Antennas and Propagat.*, Vol. 42, 311–319, 1994.

3. Melamed, T., "Phase-space Green's functions for modeling time-harmonic scattering from smooth inhomogeneous objects," *J. Math. Phys.*, Vol. 46, 2232–2246, 2004.
4. Shin, S. Y. and L. B. Felsen, "Gaussian beams in anisotropic media," *Applied Phys.*, Vol. 5, 239–250, 1974.
5. Simon, R., "Anisotropic Gaussian beams," *Opt. Commun.*, Vol. 46, 265–269, 1983.
6. Simon, R. and N. Mukunda, "Shape-invariant anisotropic Gaussian Schell-model beams: A complete characterization," *J. Opt. Soc. Am. A*, Vol. 15, 1361–70, 1998.
7. Poli, E., G. V. Pereverzev, and A. G. Peeters, "Paraxial Gaussian wave beam propagation in an anisotropic inhomogeneous plasma," *Physics of Plasmas*, Vol. 6, 5–11, Jan. 1999.
8. Perez, L. I. and M. T. Garea, "Propagation of 2D and 3D Gaussian beams in an anisotropic uniaxial medium: Vectorial and scalar treatment," *Optik*, Vol. 111, 297–306, 2000.
9. Tinkelman, I. and T. Melamed, "Gaussian beam propagation in generic anisotropic wavenumber profiles," *Optics Letters*, Vol. 28, 1081–1083, 2003.
10. Tinkelman, I. and T. Melamed, "Local spectrum analysis of field propagation in anisotropic media, Part I — Time-harmonic fields," *J. Opt. Soc. Am. A*, Vol. 22, 1200–1207, 2005.
11. Tinkelman, I. and T. Melamed, "Local spectrum analysis of field propagation in anisotropic media, Part II — Time-dependent fields," *J. Opt. Soc. Am. A*, Vol. 22, 1208–1215, 2005.
12. Khatkevich, A. G., "Propagation of pulses and wave packets in dispersive gyrotropic crystals," *J. Appl. Spectrosc.*, Vol. 46, 203–207, 1987.
13. Melamed, T. and L. B. Felsen, "Pulsed beam propagation in lossless dispersive media, Part I: Theory," *J. Opt. Soc. Am. A*, Vol. 15, 1268–1276, 1998.
14. Melamed, T. and L. B. Felsen, "Pulsed beam propagation in lossless dispersive media, Part II: A numerical example," *J. Opt. Soc. Am. A*, Vol. 15, 1277–1284, 1998.
15. Melamed, T. and L. B. Felsen, "Pulsed beam propagation in dispersive media via pulsed plane wave spectral decomposition," *IEEE Trans. Antennas and Propagat.*, Vol. 48, 901–908, 2000.
16. Kiselev, A. P., "Localized light waves: Paraxial and exact solutions of the wave equation (a review)," *Opt. Spectrosc.*, Vol. 102, 603–622, 2007.
17. Maciel, J. J. and L. B. Felsen, "Systematic study of fields due

to extended apertures by Gaussian beam discretization," *IEEE Trans. Antennas and Propagat.*, Vol. 37, 884–892, 1989.

18. Steinberg, B. Z., E. Heyman, and L. B. Felsen, "Phase space beam summation for time-harmonic radiation from large apertures," *J. Opt. Soc. Am. A*, Vol. 8, 41–59, 1991.
19. Shlivinski, A., E. Heyman, A. Boag, and C. Letrou, "A phase-space beam summation formulation for ultra wideband radiation," *IEEE Trans. Antennas and Propagat.*, Vol. 52, 2042–2056, 2004.
20. Shlivinski, A., E. Heyman, and A. Boag, "A pulsed beam summation formulation for short pulse radiation based on windowed radon transform (WRT) frames," *IEEE Trans. Antennas and Propagat.*, Vol. 53, 3030–3048, 2005.
21. Steinberg, B. Z., E. Heyman, and L. B. Felsen, "Phase space beam summation for time dependent radiation from large apertures: Continuous parametrization," *J. Opt. Soc. Am. A*, Vol. 8, 943–958, 1991.
22. Melamed, T., "Phase-space beam summation: A local spectrum analysis for time-dependent radiation," *Journal of Electromagnetic Waves and Applications*, Vol. 11, No. 6, 739–773, 1997.
23. Melamed, T., "Exact beam decomposition of time-harmonic electromagnetic waves," *Journal of Electromagnetic Waves and Applications*, Vol. 23, No. 8–9, 975–986, 2009.
24. Hadad, Y. and T. Melamed, "Non-orthogonal domain parabolic equation and its Gaussian beam solutions," *IEEE Trans. Antennas and Propagat.*, Vol. 58, accepted for publication, 2010.
25. Hoppe, D. J. and Y. Rahmat-Samii, "Gaussian beam reflection at a dielectric-chiral interface," *Journal of Electromagnetic Waves and Applications*, Vol. 6, No. 1–4, 603–624, 1992.
26. Ianconescu, R. and E. Heyman, "Pulsed beam diffraction by a perfectly conducting wedge. Exact solution," *IEEE Trans. Antennas and Propagat.*, Vol. 42, 1377–1385, 1994.
27. Heyman, E. and R. Ianconescu, "Pulsed beam diffraction by a perfectly conducting wedge. Local scattering models," *IEEE Trans. Antennas and Propagat.*, Vol. 43, 519–528, 1995.
28. Pascal, O., F. Lemaitre, and G. Soum, "Paraxial approximation effect on a dielectric interface analysis," *Ann. Telecommun.*, Vol. 51, 206–218, 1996.
29. Pascal, O., F. Lemaitre, and G. Soum, "Dielectric lens analysis using vectorial multimodal Gaussian beam expansion," *Ann. Telecommun.*, Vol. 52, 519–528, 1997.
30. Dou, W. B. and E. K. N. Yung, "Diffraction of an electromagnetic

beam by planar structures," *Journal of Electromagnetic Waves and Applications*, Vol. 15, No. 11, 1539–1549, 2001.

31. Sakurai, H. and S. Kozaki, "Scattering of a Gaussian beam by a radially inhomogeneous dielectric sphere," *Journal of Electromagnetic Waves and Applications*, Vol. 15, No. 12, 1673–1693, 2001.
32. Anastassiu, H. T. and P. H. Pathak, "Closed form solution for three-dimensional reflection of an arbitrary Gaussian beam by a smooth surface," *Radio Science*, Vol. 37, 1–8, 2002.
33. Katsav, M. and E. Heyman, "A beam summation representation for 3-D radiation from a line source distribution," *IEEE Trans. Antennas and Propagat.*, Vol. 56, 602–605, 2008.
34. Katsav, M. and E. Heyman, "Gaussian beams summation representation of half plane diffraction: A full 3-D formulation," *IEEE Trans. Antennas and Propagat.*, Vol. 57, 1081–1094, 2009.
35. Norris, A. N., "Complex point-source representation of real sources and the Gaussian beam summation method," *J. Opt. Soc. A.*, Vol. 3, 205–210, 1986.
36. Heyman, E. and L. B. Felsen, "Gaussian beam and pulsed beam dynamics: Complex-source and complex spectrum formulations within and beyond paraxial asymptotics," *J. Opt. Soc. Am. A*, Vol. 18, 1588–1611, 2001.
37. Heyman, E. and T. Melamed, "Certain considerations in aperture synthesis of ultrawideband/short-pulse radiation," *IEEE Trans. Antennas and Propagat.*, Vol. 42, 518–525, 1994.
38. Heyman, E. and T. Melamed, "Space-time representation of ultra wideband signals," *Advances in Imaging and Electron Physics*, Vol. 103, 1–63, Elsevier, 1998.
39. Kravtsov, Y. A. and Y. L. Orlov, *Geometrical Optics of Inhomogeneous Media*, Springer-Verlag, 1991.